Chinese Journal of Aeronautics 24 (2011) 127-135

Contents lists available at ScienceDirect

Chinese Journal of Aeronautics

journal homepage: www.elsevier.com/locate/cja

A New Single-blade Based Hybrid CFD Method for Hovering and Forward-flight Rotor Computation

SHI Yongjie*, ZHAO Qijun, FAN Feng, XU Guohua

National Key Laboratory of Rotorcraft Aeromechanics, Nanjing University of Aeronautics and Astronautics, Nanjing 210016, China

Received 16 April 2010; revised 18 June 2010; accepted 13 December 2010

Abstract

A hybrid Euler/full potential/Lagrangian wake method, based on single-blade simulation, for predicting unsteady aerodynamic flow around helicopter rotors in hover and forward flight has been developed. In this method, an Euler solver is used to model the near wake evolution and transonic flow phenomena in the vicinity of the blade, and a full potential equation (FPE) is used to model the isentropic potential flow region far away from the rotor, while the wake effects of other blades and the far wake are incorporated into the flow solution as an induced inflow distribution using a Lagrangian based wake analysis. To further reduce the execution time, the computational fluid dynamics (CFD) solution and rotor wake analysis (including induced velocity update) are conducted parallelly, and a load balancing strategy is employed to account for the information exchange between two solvers. By the developed method, several hover and forward-flight cases on Caradonna-Tung and Helishape 7A rotors are performed. Good agreements of the loadings on blade surface with available measured data demonstrate the validation of the method. Also, the CPU time required for different computation runs is compared in the paper, and the results show that the present hybrid method is superior to conventional CFD method in time cost, and will be more efficient with the number of blades increasing.

Keywords: hybrid CFD method; Euler equations; full potential equations; wake model; rotor; helicopters

1. Introduction

The flow around helicopter rotor blades is highly complex and characterized by flow phenomena such as shock waves on the advancing blade tip and stalls and separated flow regions at the retreating side. Additionally, a rotor blade always operates in the shed and trailed wake from other blades as well as itself. The interaction between blade and rotor wake occurring at low-speed flight condition also makes the flow more complex and challenging to predict the blade aerodynamic loads.

In the 1970s, computational fluid dynamics (CFD) technology was first applied to the rotorcraft research and significant improvements were achieved during the past several decades[1]. There are mainly two methodologies that are used for wake computation in rotor CFD analysis. One is the so-called Eulerian method, which models the whole rotor system and attempts to capture the wake structure entirely from first principles. This approach was initiated in the 1980's for hovering rotors by Roberts and Murman[2]. For forward flight, several multi-block strategies (e.g., embedded or overset grid[3], deforming mesh[4], and multi-zone methodologies[5]) are usually employed to account for the actual blade flapping, pitching and lagging motions. Although the direct wake capturing method eliminates the need for external wake models, the numerical dissipation inherent in finite volume and finite

*Corresponding author. Tel.: +86-25-84892117.
E-mail address: shiyongjie@nuaa.edu.cn
Foundation item: National Natural Science Foundation of China (10872094)

doi: 10.1016/S1000-9361(11)60016-2

difference schemes causes the vortices in the flow field to diffuse at a faster rate than that of physical diffusion. To capture the rotor far-wake well, some algorithms, such as grid refinement, unstructured grids and high-order-accuracy differencing, have appeared in recent researches[6-8], but it seems that none of these algorithms have yet been demonstrated to be able to capture the rotor wake with sufficient resolution. Furthermore, huge computation resource and time needed in solution also become barriers for conventional method (wake capturing) to be used in helicopter industry.

An alternative methodology of reducing execution time for flow computation resorts to including the external vortex wake into the CFD calculations. In this approach, the geometry of the vortex wake is obtained by using Lagrangian based wake analysis. Some wake coupling methods have been developed and coded by the previous researchers. For example, Agarwal[9] and Cao[10], et al. coupled Euler with free-wake method to compute the flow field of a helicopter in hover, and the effects of the vortex wake on blade use an equivalent angle of attack. Algermissen, et al.[11] specified the induced velocity field as a far field boundary condition for Euler equations, and applied this method to the forward flight of a five-bladed rotor. Despite the inherent theoretical discrepancy of its linear-non-linear coupling in these methods, the results are shown to agree well with measured data under most flight conditions except for the presence of strong blade-vortex interaction.

In all of the above methods, the loose coupling schemes are used, i.e., the circulation strengths of rotor wake are obtained through the unsteady vortex lattice model rather than CFD solution. It may degrade the accuracy of the vortex strength evaluating and influence the loading prediction on blade ultimately. In addition, all of these approaches solve the Navier-Stokes/Euler equations throughout the blade grid. Although the Navier-Stokes/Euler solvers can capture strong shock wave and predict air-loadings well, the use of them in the region outside the boundary layer is costly because the flow is irrotational and viscous effect is negligible[12]. An unsteady, compressible full potential analysis can be used in this region to reduce the executing time costing. Ref.[13] firstly developed such hybrid method. In their work, the spatial position of rotor wake in potential region is obtained by Eulerian approach. It improves the calculation of aerodynamic loading on blade surface due to well captured wake geometry. However, a complicated and computationally expensive algorithm is needed for donor cell search and velocity interpolation for wake marker. In forward flight, a large-scale background grid is needed to capture far wake and it increases the computation time.

To develop a high efficient computational method that can be used for rotor design application, a new single-blade based hybrid method, combing the Euler, full potential equations (FPEs) and Lagrangian based external wake is proposed to predict the aerodynamic loading for hovering and forward-flight rotors in this paper. The method solves Euler equation around the near field of blade to capture the near-wake effects and non-linear flow phenomena. An efficient and economic full-potential solver is employed to model the isentropic potential flow region far away from the blade, and the wake effects of other blades are included as an induced inflow distribution using an external wake in potential region.

The wake induced velocity on each grid point in potential zone is needed to update per time step in computation. To further reduce the CPU time, the CFD solution and rotor wake analysis are conducted parallelly, and a load balancing strategy is employed to account for information exchange between the two solvers. Comparisons between computed and measured surface pressure and sectional lift on the Caradonna-Tung and Helishape 7A rotors are presented. The results show that the presented hybrid method is highly efficient in computational time and maintains good accuracy.

2. Computational Method

The single-blade based hybrid CFD method developed in this work consists of a Euler solver, a potential solver and an external wake solver. The flow field is divided into three zones, as shown in Fig.1: 1) the near field zone in which the Euler solver is employed to predict the aerodynamic loading on the blade surface, capture the vorticity evolution and simulate the transonic flow phenomena, 2) the potential flow zone which transports the disturbance waves produced in the vicinity of the blade to the farfield, and introduces the far field boundary condition, and 3) a Lagrangian wake approach is implemented as part of the hybrid methodology to capture the effects of the tip vortex once it leaves the Euler zone, and convect it to the farfield in the inviscid zone.

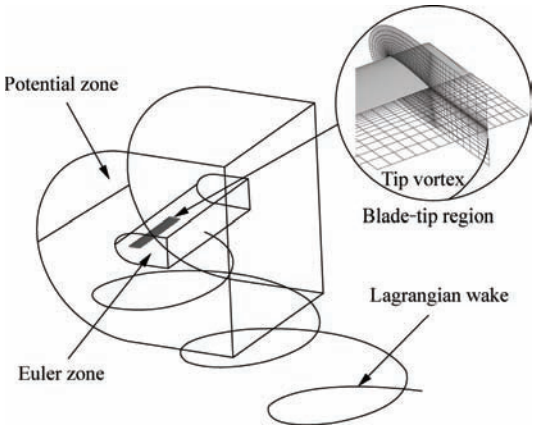

Fig.1 Schematic of three zones of flow field.

2.1. Euler solver

A Euler solver is employed to simulate the unsteady

flow field around the blade. The governing equations in Cartesian coordinate system can be written as

$$\frac{\partial}{\partial t}\iiint_V \boldsymbol{w}\mathrm{d}V + \oiint_S \boldsymbol{H}\cdot\boldsymbol{n}\mathrm{d}S = \boldsymbol{0} \tag{1}$$

where $\boldsymbol{w}$ is conserved variables vector, $\boldsymbol{H}$ inviscid flux matrix, V cell volume, S face area, and $\boldsymbol{n}$ normal vector. All physical quantities above are non-dimensionalized by rotor tip velocity v_T, air density ρ and blade chord c.

In the solver, cell-centered symmetric finite volume scheme[14] is used for spatial discretization.

The dual-time method[15] implemented by Jameson is employed to solve unsteady solution of governing equation. Eq.(1) can be replaced by

$$\frac{\partial \boldsymbol{w}^*}{\partial \tau} + \frac{3\boldsymbol{w}^* - 4\boldsymbol{w}^m + \boldsymbol{w}^{m-1}}{2\Delta t} = \frac{1}{V}\boldsymbol{R}(\boldsymbol{w}^*) \tag{2}$$

where Δt is physical time step, τ pseudo time, m physical time level, and $\boldsymbol{R}(\boldsymbol{w}^*)$ residual term.

A 5-stage Runge-Kutta scheme is used for the solution of the pseudo-time problem. However, Arnone, et al.[16] pointed out that the explicit multistage scheme becomes unstable when the physical time step Δt is of the order of the pseudo time step $\Delta\tau$ or smaller due to the term $3\boldsymbol{w}^*/(2\Delta t)$. In the present work, an implicit treatment of the term suggested by Venkatakrishnan, et al.[17] is used to ensure the numerical stability for any physical time step.

2.2. Potential flow solver

Three-dimensional unsteady potential flow problem is governed by the following equations in the Cartesian coordinate system:

$$\frac{\partial}{\partial t}\iiint_V \rho\mathrm{d}V + \oiint_S \rho\boldsymbol{v}\cdot\boldsymbol{n}\mathrm{d}S = 0 \tag{3}$$

where $\boldsymbol{v}$ is the flow velocity which is made up of four components: free stream velocity $\boldsymbol{v}_\infty$, disturbance potential velocity $\nabla\phi$, induced velocity $\boldsymbol{v}_w$ and blade moving velocity $\boldsymbol{q}_b$.

$$\boldsymbol{v} = \boldsymbol{v}_\infty + \nabla\phi + \boldsymbol{v}_w - \boldsymbol{q}_b \tag{4}$$

Eq.(3) is solved by using central difference scheme in spatial discretization and strongly implicit procedure in temporal direction, and the latter is studied by Sankar, et al.[18].

2.3. Wake model

For a rotor in flight, its blade often operates in the wake generated by vortices trailed by other blades as well as from itself. This additional effect has to be carefully modeled to get a good estimate of sectional aerodynamic loads for a rotor blade. In the current work, two wake models are used to account for the wake effects in the potential flow zones.

To avoid the double counting of wake effects on rotor blade, the velocity induced by far wake should be imposed only on the interface for Euler zone, and the first vortex element marker must be placed at the downstream interface between the Euler and the full-potential zones (see close-up view of blade-tip in Fig.1).

The Landgrebe wake model[19] established from experimental measurement is used for hovering rotor. The tip vortex geometry is described by

$$z_v = \begin{cases} k_1\psi_w & 0 \le \psi_w \le 2\pi/N_b \\ (z_v)_{\psi_w = 2\pi/N_b} + k_2(\psi_w - 2\pi/N_b) & \psi_w > 2\pi/N_b \end{cases} \tag{5}$$

where z_v is wake coordinate in axial (z direction), N_b the number of blades, ψ_w wake age, and k_1 and k_2 are empirical factors.

For forward flight, the classical Beddoes distorted wake model[20] is used to model the tip wake structure. The tip vortex geometry is given by

$$\left.\begin{aligned} x_v &= r_v\cos\psi_v + \mu_x\psi_v \\ y_v &= r_v\sin\psi_v \\ z_v &= \mu_z\psi_v + \int_0^{\psi_v}(v_z/v_T)\mathrm{d}\psi \end{aligned}\right\} \tag{6}$$

where x_v and y_v are wake coordinates in longitudinal (x direction) and lateral (y direction); ψ_v is the azimuthal angle when vortex element is formed, ψ the azimuthal angle of blade, and μ_i ($i = x, y, z$) the non-dimensional flow velocity.

The wake induced velocity at all nodes in potential zone is evaluated by the Biot-Savart law. To eliminate the singularity that occurs when the vortex line is close to the computational node, a vortex core model[21] is employed, which can be expressed by

$$v_\theta = \frac{\Gamma}{2\pi}\cdot\frac{r}{(r^2 + a_0^2)} \tag{7}$$

where v_θ is the tangential velocity, r the radial distance from the center, a_0 the core radius, and Γ the circulation strength. An empirical viscous diffusion model is used to account for the core radius growth with wake age.

$$a_0 = 0.085\,5\sqrt{\delta\nu\frac{\psi_w}{\Omega}} \tag{8}$$

where δ and ν are turbulence viscous coefficient and dynamic viscous coefficient respectively, and their values are taken from Ref.[21]; Ω is rotation speed of rotor.

2.4. Strength of bound vortex and tip vortex

In wake model, the effects of other blades are modeled by a series of bound vortex and tip vortex. The circulation strengths are computed using the sectional lift coefficient integrated from the pressure distributions obtained from the CFD solution of the flow around the blade surface. The bound vortex strength is

given by Kutta-Joukowski theorem

$$\rho v_{\mathrm{l}} \Gamma b = \frac{1}{2}\rho v_{\mathrm{l}}^2 c b C_L \tag{9}$$

where C_L is the sectional lift coefficient, b blade segment width, and v_{l} local flow velocity.

The strength of the tip vortex is taken to be the bound circulation at a predefined tip radial station ($0.98R$ is used in this work, and R is the radius of rotor) and is allowed to change from one time step to the next as the loading on the blade changes.

At the start of the simulation, the tip vortex circulations at every azimuthal position are initialized using the following formula[13]:

$$\Gamma_{\max}(\psi) = \frac{1}{2} C_T \frac{\pi}{N_{\mathrm{b}}} \cdot \frac{\sqrt{1-a^2}}{\dfrac{\pi}{16} + \dfrac{4}{9k}\left(\sqrt{1-a^2}-1\right)} \cdot \frac{1}{1+a\sin\psi} \tag{10}$$

where $k = 0.982$, $a = 1.5k\mu$, μ is the advance ratio, and C_T the thrust coefficient.

2.5. Boundary conditions

Three types of boundary conditions are required in the present hybrid method.

(1) Solid surface boundary conditions

The non-penetration conditions are enforced on the blade surface, namely the normal velocity v_n=0. The pressure p on the blade surface is computed by solving the normal momentum equation $\partial p/\partial n$=0.

(2) Far field boundary conditions

The far field surfaces exist in both Euler and full potential zones. Non-reflection conditions are implemented on the far field boundary in the Euler zone, and non-disturbation conditions in the full potential zone, hence the velocity potential is set to be zero on the outer surfaces of the full potential zone.

(3) Boundary conditions for interface between the Euler and full potential zones

The interface between the Euler and full potential zones must be carefully dealt with to allow three types of waves (acoustic, vorticity and entropy) to propagate out to the far field without false reflections. A single block O-H grid is used as computational domain in the present work, which can be conveniently divided into different zones by using one grid surface. The grid surface $j = j_{\mathrm{match}}$ is chosen as the interface between different computational domains, and $j \le j_{\mathrm{match}}$ is the Euler zone, $j \ge j_{\mathrm{match}}$ the full potential zone, where j_{match} is the match surface.

The Euler equation is solved using cell-centered finite volume scheme for spatial discretizaiton, but the finite difference method in which the flow value is stored on the grid node is used for full potential zone, so two layers must be overlapped on the either side of the match surface to transfer flow information between two zones. For Euler zone, firstly, it is necessary to search the eight nodes for the considered cell, then the flow variables at the center of the cell is obtained by interpolating from the eight nodes. The velocity components at interface $j = j_{\mathrm{match}}$ are found by adding potential and wake-induced velocities, i.e.

$$\left.\begin{aligned} u &= \phi_\xi \xi_x + \phi_\eta \eta_x + \phi_\zeta \zeta_x + u_{\mathrm{v}} \\ v &= \phi_\xi \xi_y + \phi_\eta \eta_y + \phi_\zeta \zeta_y + v_{\mathrm{v}} \\ w &= \phi_\xi \xi_z + \phi_\eta \eta_z + \phi_\zeta \zeta_z + w_{\mathrm{v}} \end{aligned}\right\} \tag{11}$$

where ξ, η and ζ are three coordinates in computational space, ϕ is velocity potential.

Then the pressure and density values are computed using the corresponding formulae.

For the full potential zone, the velocity is the only necessary information to obtain from the Euler zone. Since the full potential zone is the non-vorticity flow field, it must be noted that transferring vorticity to the full potential zone is avoided. So the boundary condition on the interface for the full potential zone can be given as

$$\phi_n = (\boldsymbol{v}_{\mathrm{EULER}} - \boldsymbol{v}_w) \cdot \boldsymbol{n} \tag{12}$$

where ϕ_n is the normal derivative of ϕ, $\boldsymbol{v}_{\mathrm{EULER}}$ the velocity vector solved by Euler equations.

3. Results and Discussion

To validate the hybrid solver developed for rotor flow field computations in hover and forward flight, several cases for Caradonna-Tung rotor and Helishape 7A rotor have been tested and compared with the available measured data.

The Caradonna-Tung rotor is a 2-bladed, untwisted and rectangular platform. The blades have NACA 0012 sections and an aspect ratio of 6[22]. The 7A rotor is 4-bladed, articulated with 2.1 m radius, 0.14 m chord, and has a non-constant geometric twist, and consists of OA213, OA209 airfoil sections along span[23].

3.1. Computation specifics

An O-H grid with 131 chordwise points, 53 spanwise points and 51 points in the normal direction is used as computational domain for both Caradonna-Tung and Helishape 7A rotors in computations. The domain extends approximately half radius normal to the blade surface and one radius beyond the blade tip. About 39.2% of the grid points fall into Euler zone. The Euler zone covers about half-chord around the blade.

In the present method, the hover and forward flight calculations are treated in the same way. To obtain good resolutions of loading time-history on blade surface, the results are presented after 3 revolutions. In every revolution, the unsteady computations are performed for a rotor azimuthal increment of 0.25° (1 440 azimuthal stations) with 20 Runge-Kutta subiterations per time step.

The results of hybrid method may also be affected by the number of wake revolutions and segments in every revolution wake. In the presented solver, totally

144 wake segments (with 6 wake revolutions and 24 segments in one revolution) are used to calculate the wake induced velocity.

3.2. Caradonna-Tung rotor

The Caradonna-Tung rotor has been tested for several non-lifting and lifting cases. Surface pressure data is presented at a number of chordwise locations at several stations for code validation.

3.2.1. Non-lifting cases

The solver is firstly applied to a non-lifting case, the tip mach number Ma_{tip}=0.52, collective angle $\theta = 0°$, where no wake modeling is needed. Fig.2 presents surface pressures on the blade at r/R=0.89, 0.96. In Fig.2, C_p is the surface pressure coefficient. The computed results agree well with measured data[22]. The density and pressure contours at r/R=0.89 are also shown in Fig.3. In Fig.3, the Euler/full-potential interface is drawn for clarity. It can be seen that both of the contours go smoothly through the interface, which indicates the successful treatment of interface boundary condition for the two coupling zones.

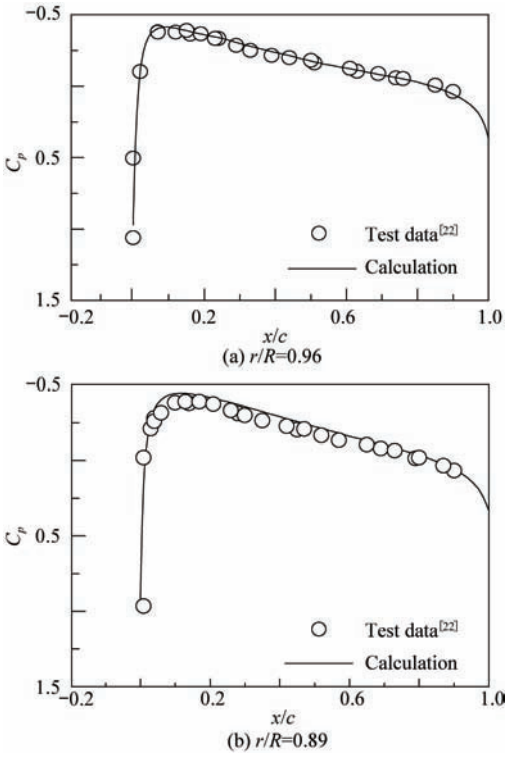

Fig.2 Surface pressure coefficient for non-lifting hover.

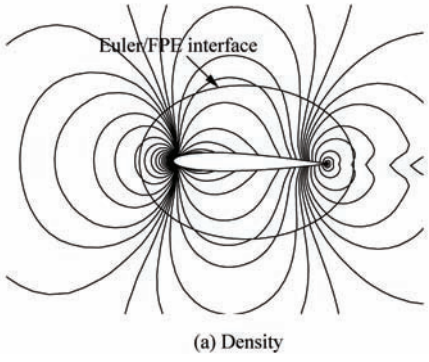

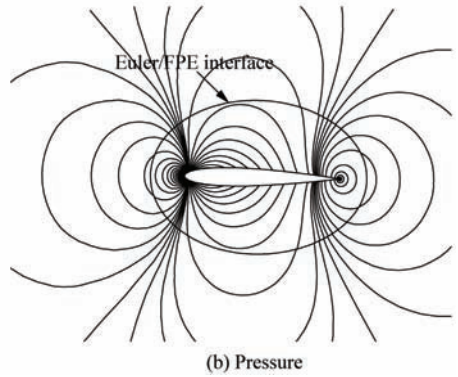

Fig.3 Contour plots of flow field at r/R=0.89.

Fig.4 compares computed surface pressure with measured values at r/R=0.89 for non-lifting forward flight. The test was conducted at Ma_{tip}=0.8, $\mu = 0.2$. The maximum local Mach number reaches 0.96 at advancing side, the outer portions of blade are in transonic flow and strong shock wave exists on both upper and lower surfaces of blade. Although this is difficult to simulate, the predicted pressures correlate well with

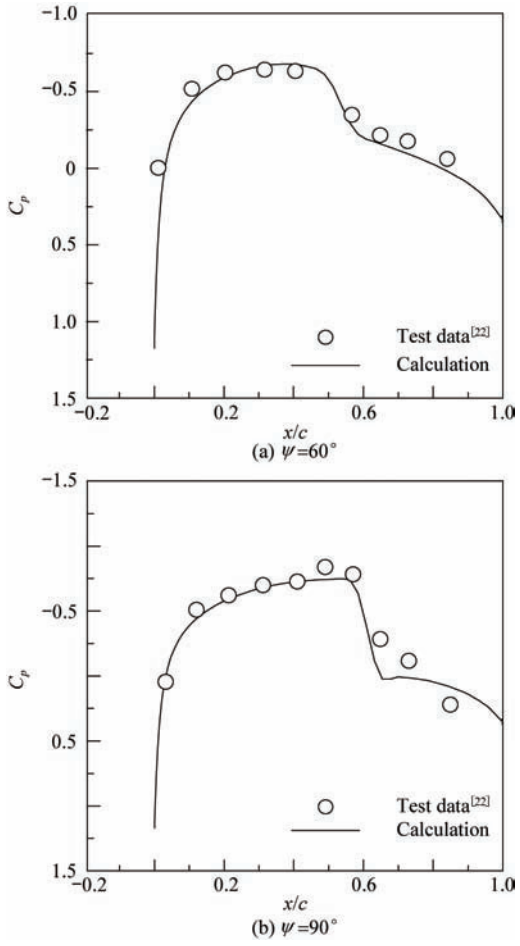

Fig.4 Surface pressure coefficient for non-lifting forward-flight (r/R =0.89).

the measured data[22]. All of the above results show that the present hybrid method can be successfully applied to transonic flows.

3.2.2. Lifting hover case

In this section, the loads on a hovering rotor with and without wake model are presented to validate the wake coupling method. The wake induced velocities at all grid points need to be recalculated at every time step so as to be consistent with CFD solver. However, for hover cases, the flow field is quasi-steady and the induced velocity on blade surface does not change with azimuthal angle. In computation, the coefficients of induced velocity at grid points are computed and stored only one time, and the values at other azimuthal positions are obtained by rotating transformation.

Fig.5 shows the chordwise pressure distributions at two radial stations with comparisons to experimental data[23]. The run case is Ma_{tip}=0.439, with a collective pitch of 8°. As expected, the pressure is overestimated drastically if wake effects are neglected. When tip vortex is included, the loads are predicted accurately compared to the measured data.

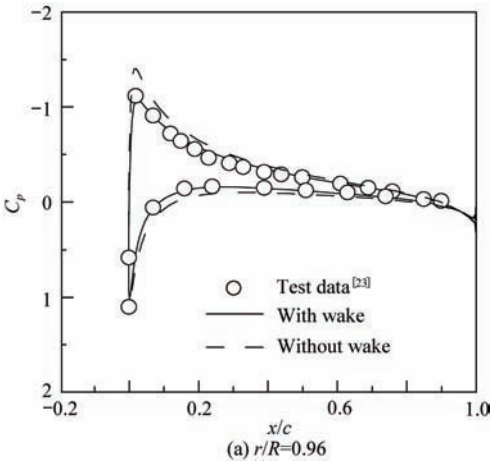

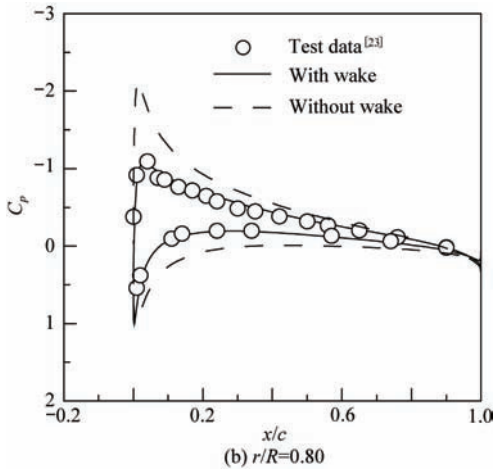

Fig.5 Surface pressure coefficient in lifting hover case.

Table 1 shows the CPU time usage of the present hybrid method compared with that of the conventional overset method. It is noted that, in conventional method, one blade is needed to solve in blade rotation coordinate for hover cases. A typical hover solution requires about 4.76 h of CPU time for hybrid method and 8.88 h for conventional method on PC (Core2 E 7200 2.6 G). About 46.4% CPU time can be reduced. For forward flight solution, approximately 51.5% and 73.1% CPU time reductions are achieved with and without parallel method. It indicates that the present single-blade based hybrid method is superior in computation time and more time can be reduced with parallel computation.

Table 1 Comparison of CPU time for conventional and hybrid CFD methods

Parameter		Hybrid method	Conventional overset method
Grid		354 000	200 000 for one blade; 300 000 for background
Computation time/s		Euler solver: 8.8 FPE: 3.1 Wake calculation: 9.6	Hover: 22.2 Forward flight: 44.3
Total CPU time/h	Hover	4.76	8.88
	Forward flight	Without parallel: 25.8 With parallel: 14.3	53.16

3.3. Helishape 7A rotor

In this section, the hover and forward flight cases of the 7A rotor with complicate aerodynamic shape are also presented to validate the hybrid method.

3.3.1. Effects of wake model in hover

Fig.6 shows the chordwise surface pressure distribution for 7A rotor at Ma_{tip}=0.617, C_T=0.005 87, with a built-in collective pitch of 8.94° at 70% of rotor radius[23]. For Beddoes wake model, it gives the rigid wake without contraction for hover case, which causes larger downwash at the outer portion of rotor, thus the blade loading is reduced. The Landgrebe wake model, in the meantime, reduces velocity at outer portion of rotor and even induces the upwash at tip region due to wake contraction. So the predicted loadings on blade surface

agree well with measured data[23]. It means that the accuracy of predicted aerodynamic loadings is associated with wake model, and the good resolution of rotor flow can be achieved with reasonable wake geometry.

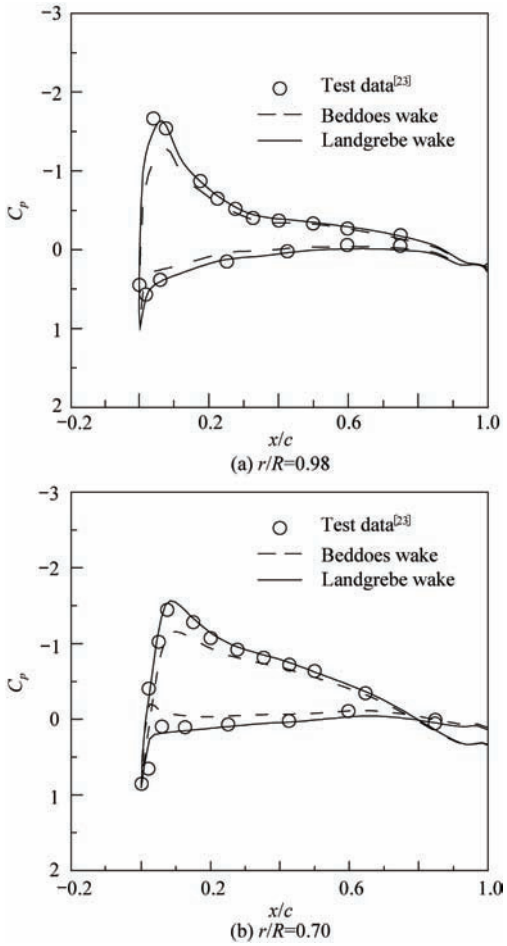

Fig.6 Surface pressure coefficient of 7A rotor in hover.

3.3.2. 7A rotor in forward flight

In forward flight, the tip vortices convect downward and afterward with local velocity, so large-scale background mesh is needed to capture rotor wake in conventional overset-grid method. However, for single blade computation, only one body-fitted grid around blade is required, and the influence of other blades is modeled as a collection of bound and tip vortices.

The hybrid solver is applied to a low-speed forward-flight case, with Ma_{tip}=0.617 and μ=0.167. The flow field exhibits a strong interaction between the blade and the wake system, and is highly unsteady under this flight condition. The motions of cyclic pitching and flapping are from test[23].

Fig.7 shows the spanwise sectional lift coefficient time-histories at two radial stations. The sectional lift is predicted well except for the phase error in the range of 135°-180°. It may be caused by the neglect of blade elastic deformations.

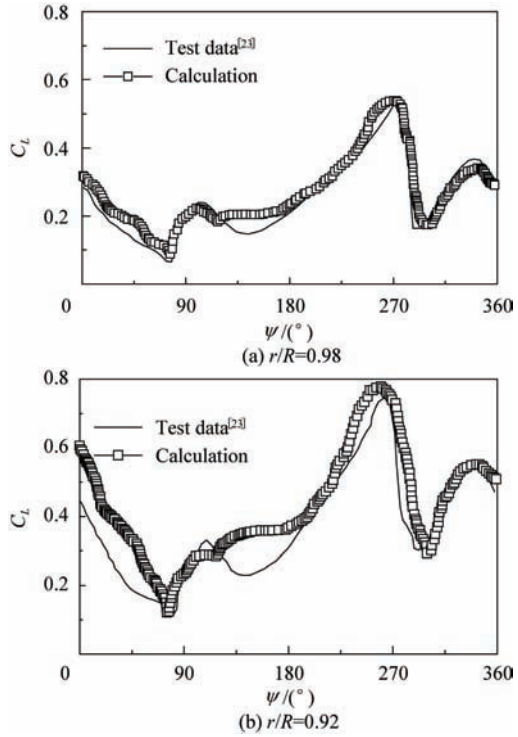

Fig.7 Sectional lift coefficient of 7A rotor in forward flight.

Fig.8 compares the chordwise pressure coefficients with the experiment data[23]. It is seen that, a good agreement is achieved at all azimuthal positions, and

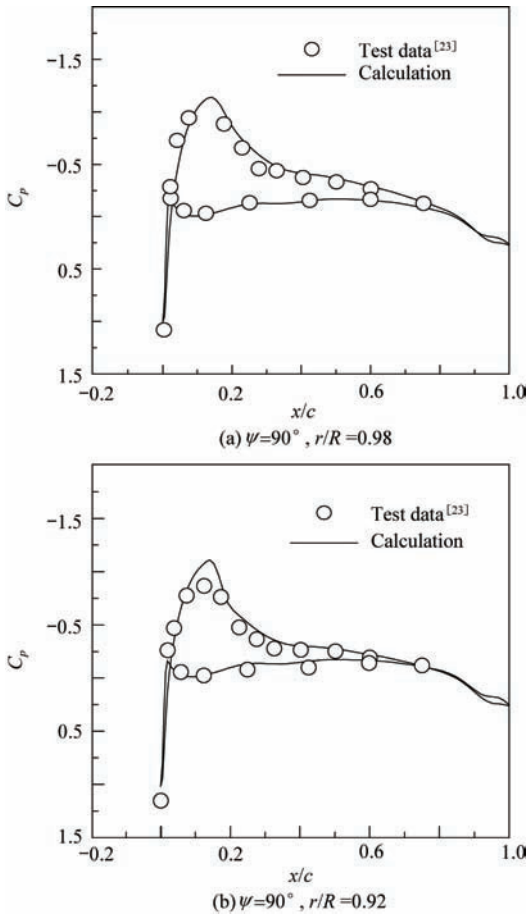

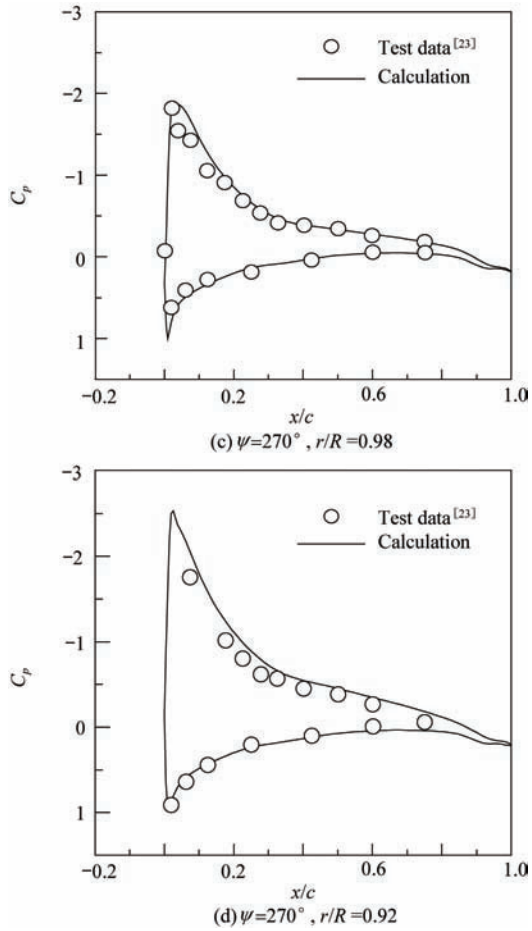

Fig.8 Surface pressure coefficient of 7A rotor in forward flight.

the results at r/R=0.98 are better than those at r/R= 0.92. However, the predicted results are somewhat overestimated at azimuthal 270°. The discrepancies may relate to the level of non-linear aerodynamic and wake model used in the method. The viscous effects, which account for flow phenomena of dynamic stall at retreating side, should be included and free wake model should be better coded to the solver in future studies.

Table 2 shows the comparison of CPU time for 4-bladed 7A rotor. It should be pointed out that the CPU time required is the same as 2-bladed Caradonna-Tung rotor for hover case, which is not presented in Table 2. A typical forward-flight case requires 15.4 h for hybrid method, and 83.68 h for conventional method. Approximately 81.6% CPU time reduction is achieved. It is expected that more CPU time reduction with the present method will be reached when the rotor has more number of blades.

Table 2 Comparison of CPU time for 7A rotor in forward flight

Parameter	Hybrid method	Conventional overset method
Computation time/s	Euler solver: 8.8 FPE: 3.1 Wake calculation: 17.6	69.74
Total CPU time/h	15.4 (3 revolutions)	83.68 (3 revolutions)

4. Conclusions

A new hybrid Euler/full potential/Lagrangian wake model solver is developed in this work for hovering and forward-flight rotors. The solver is applied to several cases for different rotors. From the results presented in this paper, the following conclusions can be drawn:

(1) The present method is not only suitable for solving transonic flow in high-speed forward flight, but also for blade vortex interaction (BVI) capturing in low-speed forward flight. Furthermore, the accuracy of aerodynamic loadings on blade surface is associated with wake model, and good result can be achieved with reasonable wake geometry.

(2) Compared to conventional CFD method, the present single-blade based hybrid method is superior in computation time. For a typical hover case, about 46.4% CPU time reduction can be achieved, while for forward-flight case, more than 70% CPU time can be reduced, and the method is more efficient as the number of blades increases.

(3) With the concept of parallel computation, the CFD solver and rotor wake solver can be run independently with each other, and CPU time is reduced apparently. For a forward-flight rotor, about additional 26% CPU time can be reduced.

In the future studies, Navier-Stokes equations will be used to account for the viscous effects in the region surrounding the blade and more advanced free-wake models will be coupled into the CFD solver instead of the prescribed wake. All these measures will improve the prediction of aerodynamic loadings on blade surface. In addition, a rotor trim procedure will also be employed to achieve actual collective, cyclic pitching and blade flapping motion.

References

[1] Strawn R C, Caradonna F X, Duque E P N. 30 years rotorcraft computational fluid dynamics research and development. Journal of the American Helicopter Society 2006; 51(1): 5-21.

[2] Roberts T W, Murman E M. Solution method for hovering helicopter rotor using the Euler equations AIAA-1985-0436, 1985.

[3] Ahmad J, Duque E P N. Helicopter rotor blade computation in unsteady flows using moving overset grids. Journal of Aircraft 1996; 33(1): 54-60.

[4] Boniface J C, Mialon B, Sides J. Numerical simulation of unsteady Euler flow around multibladed rotor in forward flight using a moving grid approach. American Helicopter Society 51st Forum. 1995.

[5] Bangalore A, Sankar L N. Forward flight analysis of slatted rotors using Navier-Stokes methods. Journal of Aircraft 1997; 34(1): 80-86.

[6] Kang H J, Kwon O J. Unstructured mesh Navier-Stokes calculations of the flow field of a helicopter rotor in hover. Journal of the American Helicopter Society 2002; 47(2): 90-99.

[7] Kim J W, Park S H, Yu Y H. Euler and Navier-Stokes

simulations of helicopter rotor blade in forward flight using an overlapped grid solver. AIAA-2009-4268, 2009.
[8] Hanriharan N, Sankar L N. First-principles based high order methodologies for rotorcraft flowfield studies Proceedings of 55th Annual Forum of AHS. 1999; 1921-1933.
[9] Agarwal R K, Deese J E. Euler calculations for flowfield of a helicopter in hover. AIAA Journal 1987; 24(4): 231-238.
[10] Cao Y H, Yu Z Q, Su Y, et al. Combined free wake/CFD methodology for predicting transonic rotor flow in hover. Chinese Journal of Aeronautics 2002; 15(2): 65-71.
[11] Algermissen G, Wanger S. Computation of helicopter BVI noise by coupling free-wake, Euler and Kirchhoff method. AIAA-1998-2238, 1998.
[12] Bhagwat M J, Moulton M A, Caradonna F X. Development of a CFD-based hover performance prediction tool for engineering analysis. Journal of the American Helicopter Society 2007; 52(3): 175-188.
[13] Yang Z, Sankar L N, Smith M J, et al. Recent improvements to a hybrid method for rotors in forward flight. Journal of Aircraft 2002; 39(5): 804-812.
[14] Stolcis L, Johnston L J. Solution of the Euler equations on unstructured grids for two-dimensional compressible flow. Aeronautical Journal 1990; 94(936): 181-195.
[15] Jameson A. Time-dependent calculations using multigrid with applications to unsteady flows past airfoils and wings. AIAA-1991-1596, 1991.
[16] Arnone A, Liou M S, Povinelli L A. Multigrid time-accurate integration of Navier-Stokes equations. AIAA-1993-3361, 1993.
[17] Venkatakrishnan V, Mavriplis D J. Implicit method for the computation of unsteady flows on unstructured grids. Journal of Computational Physics 1996; 127(2): 380-397.
[18] Sankar L N, Prichard D. Solution of transonic flow past rotor blades using the conservative full potential equation. AIAA-1985-5012, 1985.
[19] Landgrebe A J. The wake geometry of a hovering helicopter and its influence on rotor performance[J]. Journal of the American Helicopter Society 1972; 17(4): 3-15.
[20] Beddoes T. A wake model for high resolution airloads. International Conference on Rotorcraft Reasearch. 1985.
[21] Bagai A, Leishman J G. Rotor free wake modeling using a pseudo implicit technique including comparisons with experimental data. Journal of the American Helicopter Society 1995; 40(3): 29-41.
[22] Caradonna F X, Tung C. Expermiental and analytical studies of a model helicopter rotor in hover. Vertical 1981; 5(1): 149-161.
[23] Steijl R, Barakosy G N, Badcock K J. A CFD framework for analysis of helicopter rotors. AIAA-2005-5124, 2005.

Biographies:

SHI Yongjie Born in 1983, he received his Ph.D. degree from Nanjing University of Aeronautics and Astronautics (NUAA) in 2010 and is now a lecturer in NUAA. His main research fields are helicopter aerodynamics, computational fluid dynamics and rotor aeroacoustics.
E-mail: shiyongjie@nuaa.edu.cn

ZHAO Qijun Born in 1977, he has been a professor since 2008 at Nanjing University of Aeronautics and Astronautics. His research interests are helicopter aerodynamics and rotor CFD.
E-mail: zhaoqijun@nuaa.edu.cn

FAN Feng Born in 1987, he is a Ph.D. candidate in Nanjing University of Aeronautics and Astronautics. His main research interests are rotor CFD and rotor aeroacoustics.

XU Guohua Born in 1963, he is a professor in Nanjing University of Aeronautics and Astronautics. His major research interests include helicopter aerodynamics, rotor CFD and rotor aeroacoustics.
E-mail: ghxu@nuaa.edu.cn